Dalton Transactions

Cite this: *Dalton Trans.*, 2012, **41**, 5307

www.rsc.org/dalton

PAPER

Synthesis and characterization of azolate gold(I) phosphane complexes as thioredoxin reductase inhibiting antitumor agents†

Rossana Galassi,*[a] Alfredo Burini,[a] Simone Ricci,[a] Maura Pellei,[a] Maria Pia Rigobello,[b] Anna Citta,[b] Alessandro Dolmella,[c] Valentina Gandin[c] and Cristina Marzano*[c]

Received 20th September 2011, Accepted 8th February 2012
DOI: 10.1039/c2dt11781a

Following an increasing interest in the gold drug therapy field, nine new neutral azolate gold(I) phosphane compounds have been synthesized and tested as anticancer agents. The azolate ligands used in this study are pyrazolates and imidazolates substituted with deactivating groups such as trifluoromethyl, nitro or chloride moieties, whereas the phosphane co-ligand is the triphenylphosphane or the more hydrophilic TPA (TPA = 1,3,5-triazaphosphaadamantane). The studied gold(I) complexes are: (3,5-bis-trifluoromethyl-1H-pyrazolate-1-yl)-triphenylphosphane–gold(I) (**1**), (3,5-dinitro-1H-pyrazolate-1-yl)-triphenylphosphane–gold(I) (**2**), (4-nitro-1H-pyrazolate-1-yl)-triphenylphosphane–gold(I) (**5**), (4,5-dichloro-1H-imidazolate-1-yl)-triphenylphosphane–gold(I) (**7**), with the related TPA complexes (**3**), (**4**), (**6**) and (**8**) and (1-benzyl-4,5-di-chloro-2H-imidazolate-2-yl)-triphenylphosphane–gold(I) (**9**). The presence of deactivating groups on the azole rings improves the solubility of these complexes in polar media. Compounds **1–8** contain the N–Au–P environment, whilst compound **9** is the only one to contain a C–Au–P environment. Crystal structures for compounds **1** and **2** have been obtained and discussed. Interestingly, the newly synthesized gold(I) compounds were found to possess a pronounced cytotoxic activity on several human cancer cells, some of which were endowed with cis-platin or multidrug resistance. In particular, among azolate gold(I) complexes, **1** and **2** proved to be the most promising derivatives eliciting an antiproliferative effect up to 70 times higher than cis-platin. Mechanistic experiments indicated that the inhibition of thioredoxin reductase (TrxR) might be involved in the pharmacodynamic behavior of these gold species.

Introduction

The consolidated and exceptional antitumor activity of platinum (II) compounds on the clinical treatment of different types of cancers is unfortunately accompanied by serious side effects and by the occurrence of cis-platin resistance.[1] The continuous struggle to overcome these latter drawbacks led to two other platinum based drugs oxaliplatin and carboplatin.[2] However, chemists are still seeking new and more potent metal based drugs to reach a good compromise between an optimal cytotoxic activity and minor liver and kidney toxicities, typical for these kinds of drugs.[3] Coinage metals have been taken in consideration as alternative metals in the design of metal based drugs; among them, some gold(I)complexes had success first for their efficacy against inflammatory diseases such as rheumatoid arthritis, and then for their ascertained antineoplastic activity. Simultaneously with the cytotoxicity studies, a great effort has been made to identify the molecular targets for gold(I) based drugs that are comparable to platinum based drugs, but this topic is still a challenge for researchers.[4,5] Classes of gold(I) compounds containing phosphanes as ligands[6–8] or ancillary ligands[9–13] have been studied, which are similar to the well-studied auranofin, consisting of a sugar frame bound to a gold(I) triethylphosphane ligand. Some examples of phosphane complexes, being the most active *in vivo*, reached the pre-clinical pharmacological evaluation.[14] Unfortunately, severe hepatotoxicity was verified and stopped their development. The conclusion of this promising study was that the hydro/lipophilicity balance of the gold complex is the likely key to be focused on in order to achieve the goal.[15–17] Hence, the design of gold complexes for biological testing should consider the involvement of more hydrophilic phosphane and/or other polar or more bio-compatible co-ligands. Based on these previous studies, a new class of gold(I) complexes with phosphane ligands and biomolecules such as azoles has been designed in this study. This choice was particularly important given that pyrazoles and imidazoles play a pivotal role in the coordination chemistry of gold in the +1 oxidation state. Moreover, in pyrazoles, substitution at the 3 and/or 5 position adjacent

[a]*School of Science and Technology, Chemistry Division, University of Camerino, via S. Agostino, 1, 62032 Camerino, Italy. E-mail: rossana.galassi@unicam.it; Fax: +39 737 637345; Tel: +39 737 402243*
[b]*Dipartimento di Chimica Biologica, Università di Padova, viale G. Colombo 3, 35131 Padova, Italy*
[c]*Dipartimento di Scienze Farmaceutiche, Università di Padova, via Marzolo 5, 35131 Padova, Italy*

†CCDC 847347 and 847346 for compounds **1** and **2**. For crystallographic data in CIF or other electronic format see DOI: 10.1039/c2dt11781a.

to the nitrogen atoms is particularly easy to achieve, and can strongly affect the steric environment around the N-donors and any metal ions coordinated to them.[18] Pyrazolates can coordinate as monodentate, exo-(k^2) and endo-bidentate ($k^1 : k^1$, μ). In the bridging mode, pyrazolate ligands can give rise to nine-membered cyclic trinuclear Au(I) derivatives in a rather high yield by treating the pyrazolate ligands with LAuCl precursors, where L is a labile ligand. In the literature several structures of these [μ-pz–Au_3] compounds are reported[19–21] and the success of their syntheses does not seem to be affected by the steric hindrance of the substituents in the 3, 4 and 5 positions of the pyrazole ring, as highlighted by the synthesis of cyclic [μ-pz–Au_3] compounds with a very hindered 3,5-disubstituted-pyrazolate.[22,23] However, if L in the starting gold complex is dimethylsulfide, tetrahydrothiophene or triphenylarsine ligands, dinuclear,[24,25] trinuclear[19,20] or polynuclear derivatives[26] can be obtained. On the other hand, when the gold(I) chloride precursor contains a phosphane as ligand, the exchange reaction is more difficult and mononuclear derivatives can be readily obtained.[19,27–29]

$$\mathrm{AzNa} + \mathrm{LAuCl} \Rightarrow \mathrm{AzAuL} + \mathrm{NaCl} \quad (1)$$

(Az = N-pyrazolate or N-imidazolate; L = PPh_3 or TPA = 1,3,5-triazaphosphaadamantane)

Imidazolates are heterocycles similar to pyrazolates and their coordination modes on gold(I) can lead to mononuclear[30–32] or trinuclear cyclic gold(I) complexes.[33,34] However, contrary to pyrazolates, different synthesis strategies can be adopted. Mononuclear imidazole or pyrazole phosphane Au(I) compounds have been studied for their antimicrobial activity[27] while the cytotoxic activity of phosphane Au(I) compounds and several pyridylphosphane Au(I) complexes has been ascertained and evaluated on many cancer cell panels. Moreover, phosphane complexes such as $[Au(d_2pypp)_2]Cl$ where $d_2$pypp = 1,3-bis(di-2-pyridylphosphino)propane, at sub-micromolar concentrations, selectively induce apoptosis in breast cancer cells but not in normal breast cells. Apoptosis was induced *via* the mitochondrial pathway, which involved mitochondrial membrane potential depolarisation, as well as the depletion of the glutathione pool and the activation of capsase-3 and capsase-9.[7,16,35] The mechanism of action for gold(I) phosphane complexes is still a challenge and several likely molecular targets have been identified. In general, these complexes are powerful inhibitors of thioredoxin reductase (TrxR).[5] This enzyme plays a crucial role in the intracellular redox balance and takes part in a wide variety of cell activities including cell proliferation, cell signalling, apoptosis, angiogenesis, and embryogenesis.[36] TrxR is involved in many aspects of tumor pathophysiology and many cancer cell lines and tumors exhibit increased production of TrxR. Furthermore, upregulation of TrxR has been associated with resistance to chemotherapy,[37] in addition to auranofin having been recently shown to open mitochondrial pathways to apoptosis, through the selective inhibition of mitochondrial thioredoxin reductase, even in human ovarian cancer cells resistant to cis-platin.[38]

Gold(I) derivatives with 3,5-dialkyl or diaryl pyrazolate as ligands show peculiar features in the field of emission properties[25,39] and material science,[28] while their low solubility in polar solvents makes it difficult to consider these compounds for biological testing. With the introduction of more polar groups to the pyrazole or imidazole rings, reactions between substituted-azolates and Ph_3PAuCl or TPAAuCl were carried out to obtain mononuclear gold(I) derivatives. In this study pyrazole and imidazole phosphane gold(I) compounds have been synthesized, characterized and biologically evaluated for their cytotoxic effects and for some specific enzyme inhibition actions. The azoles chosen for these complexes were pyrazoles and imidazoles containing deactivating groups (nitro-, trifluoromethyl- or halide groups) and phosphane as the co-ligands such as triphenylphosphane (PPh_3) and 1,3,5-triaza-phosphaadamantane (TPA).

The newly synthesized azolate gold(I) compounds have been tested for their antitumor properties on a wide panel of human cancer cell lines including cis-platin resistant and multidrug resistant (MDR) phenotypes. Based on the cytotoxicity screening, the most promising drug candidates, gold(I)-triphenylphosphane derivatives, have been also evaluated for their capacity to inhibit cytosolic and mitochondrial isoforms of TrxR, both *in vitro* (in a cell-free system) and in human ovarian 2008 cancer cells. In 2008 cells, the inactivation of the closely related flavoenzymes glutathione reductase (GR) and glutathione peroxidase (GPx) was also examined with the aim of proving their selectivity towards TrxR.

Table 1 List of the compounds

Compound	Formula	Yield, %	Solvents used in the synthesis
1	3,5-$pz^{CF3}AuPPh_3$	75	CH_3OH–THF
2	3,5-$pz^{NO2}AuPPh_3$	90	THF
3	3,5-pz^{CF3}AuTPA	75	CH_3CN–CH_3OH
4	3,5-pz^{NO2}AuTPA	76	CH_3OH–H_2O
5	4-$pz^{NO2}AuPPh_3$	55	THF–CH_3OH
6	4-pz^{NO2}AuTPA	59	THF–CH_3OH–CH_3CN
7	4,5-$im^{Cl}AuPPh_3$	84	CH_3OH
8	4,5-im^{Cl}AuTPA	78	CH_3OH
9	4,5-$im^{1\text{-}Bz,Cl}AuPPh_3$	40	THF

Results and discussion

Syntheses and characterizations

The list of synthesized compounds, yields and solvent conditions are reported in Table 1 and their schematic structures are shown in the Chart 1. The syntheses of complexes **1–8** have been performed by following the eqn (1) reaction scheme. Complex **9** is the only one possessing the C–Au–P environment and it was obtained by the imidazole C2-lithiation at −40 °C in THF followed by the addition of Ph_3PAuCl. The starting materials used to obtain complexes **1–8** show different solubility in most common solvents. In order to overcome this disadvantage, mixtures of solvents were sometime used. When the starting azole was neutral, the first step of the synthesis was the N–H deprotonation with methanolic NaOH or KOH (compounds **1**, **3**, **7** and **8**) or with NaH/THF (compounds **5** and **6**). The synthesis yields range from 55 to 90% with the lowest yields for complexes with 4-nitropyrazole as the ligand. Several methods and different solvents were tested to obtain a soluble product from the reaction of 3,5-dinitropyrazolate and TPAAuCl. At any rate, the scarce soluble compound **4** was obtained with a good yield.

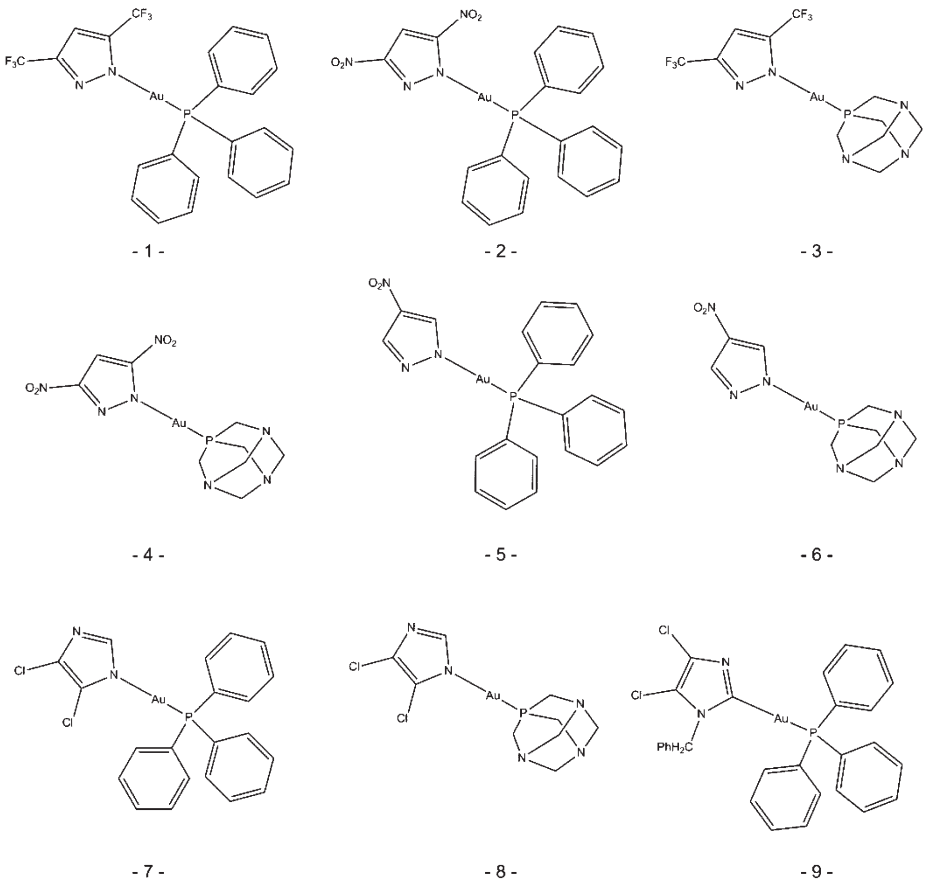

Chart 1 Schematic view of the compounds synthesized in this study.

Compounds **1–9** were characterized by elemental analysis, IR, ^{1}H and ^{31}P NMR spectroscopies and by ESI mass spectrometry. Compounds **1** and **2** were isolated as single crystals and the crystal structure determinations were performed by single-crystal X-ray Diffraction. The NMR characterization of compounds **1–9** shows the expected signals in the ^{1}H NMR spectra, and singlets in the ^{31}P NMR spectra. Substitution of the chloride with the azolate ligand does not introduce significant shifts in the ^{31}P NMR signals of the phosphane moieties. Only in the case of compound **5**, a signal broadening was observed at room temperature, which was likely due to linkage isomerism. Phosphane co-ligand fast exchange likely occurs in acetone solution. In fact, by adding a molar amount of free PPh_3 to compound **2** in the NMR tube, only a slight shift was observed (from 31.06 to 31.58 ppm). This behavior had already been observed in CD_2Cl_2 by Oda in [Au(L)PPh_3] where HL was either imidazole or pyrazole.[27] The ESI-MS characterization reveals good ionization in both positive and negative fields in acetonitrile solutions. In the former, bis-phosphanegold(I) cations were recorded for most of the complexes, while in the negative field monoanionic $(Az)_2Au$ moieties were observed. Compound **8** was not investigated by ESI due to its low solubility in CH_3CN or other ESI compatible solvents. In the IR spectra the characteristic bands for azoles were found in the range 3050–3170 cm^{-1} (C–H azole stretching), 1550–1650 cm^{-1} and 1460–1510 cm^{-1} attributable to C═C and C═N stretchings. Small shifts were also recorded for the bands attributed to the vibrational modes of NO_2, CF_3 and C–Cl groups upon coordination to the gold–phosphane moieties. The band due to P_{quat}–C_{ph} stretching is visible at 1100 cm^{-1} in all the compounds.[40]

Crystal structures descriptions

The crystal structure of complexes **1** (molecules I and II) and **2** are shown in Fig. 1. Crystal data are reported Table 2 while selected bond distances and bond angles are in Table 3. The overall shapes of the three molecules are similar and this is revealed by an inspection made with the Molecule Overlay routine in Mercury.[41] The fit of the skeleton of **2** with those of molecules I and II of **1** returns RMSDs of 0.11 and 0.06 Å, respectively.

The geometries are dictated by the linear coordination of the gold atoms, and the P–Au–N angles are 174.5(2)° in **2** and 178.0(1)° and 175.1(1)° in molecules I and II of **1**, respectively. This kind of deviation from the ideal 180° for linear coordination is not unusual for a two-coordinated gold complex. In fact, a search in the CCDC[42] database reveals that the mean P–Au–N angle is 175.4° in about 200 reported complexes. The unit cell is filled in such a way that no Au–Au interaction can be detected in either complex.

By looking at the P–Au–pyrazolate moieties, all the atoms of this fragment are coplanar within 0.10 Å in **2** and within 0.05 Å in the two independent molecules of **1**. The pyrazolate ligands themselves are almost perfectly planar in both complexes. They

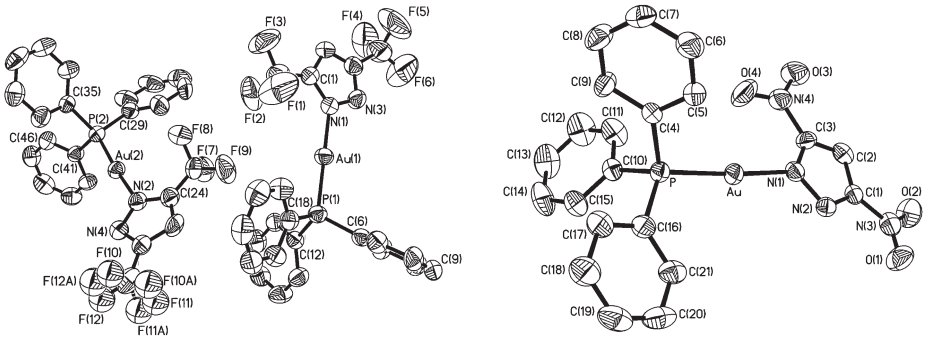

Fig. 1 ORTEP view of the complexes (**1**) (left) and (**2**) (right), together with the numbering scheme. Ellipsoids are at the 40% probability level; the hydrogen atoms have been omitted. In the view of **1**, the C-F bonds of the trifluoromethyl residue of molecule II with refined site occupancy of 0.48 have been drawn with dashed lines and the labeling has been limited for clarity.

Table 2 Crystallographic data for the two complexes (**1**) and (**2**)

	1	**2**
Empirical formula	$C_{23}H_{16}N_2F_6PAu$	$C_{21}H_{16}N_4O_4PAu$
Formula weight	662.31	616.31
Wavelength (Å)/ temperature (K)	0.71073/293(2)	0.71073/293(2)
Crystal system	Monoclinic	Monoclinic
Crystal size	0.35 × 0.15 × 0.15	0.20 × 0.15 × 0.12
Space group	$P\,2_1/c$ (No. 14)	$P\,2_1/c$ (No. 14)
a (Å)	14.633(4)	8.1300(16)
b (Å)	9.092(2)	11.393(2)
c (Å)	35.389(5)	23.339(5)
β (°)	97. 79(3)	97.60(3)
Volume (Å^3)	4664.8(17)	2142.8(7)
Z (molecules/unit cell)	8	4
Calculated density (Mg m^{-3})	1.886	1.910
Absorption coefficient, μ (cm^{-1})	6.437	6.980
F (000)	2528	1184
Independent (unique) reflections	9147	4165
Observed reflections [$I > 2\sigma(I)$]	6221	3856
Data/parameters/restraints	9147/593/0	4165/280/0
Goodness-of-fit[a] on F^2	0.932	1.364
Final R indices [$I > 2\sigma(I)$]	R_1[b] = 0.0368; wR_2[c] = 0.0891	R_1[b] = 0.0343; wR_2[c] = 0.0887
Largest difference peak and hole (eÅ^{-3})	0.991 and −0.588	0.847 and −1.085

[a] Goodness-of-fit = $[\sum(w(F_o^2 - F_c^2)^2)/(N_{obsevns} - N_{params})]^{1/2}$, based on all data; [b] $R_1 = \sum(||F_o| - |F_c||)/\sum|F_o|$; [c] $wR_2 = [\sum[w(F_o^2 - F_c^2)^2]/\sum[w(F_o^2)^2]]^{1/2}$.

are arranged in such a way that the mean plane of the ligand is close to the mean plane of one of the three phenyl rings of the PPh_3 ligands and roughly orthogonal to the remaining two. In **2**, the dihedral angles made by these planes are 9.8, 63.9, 83.6°; in **1**, the corresponding values for molecules I and II are 31.9, 69.7, 84.9° and 22.0, 69.4, 71.7°, respectively. As for the trigonal pyramidal PPh_3 moiety, it shows the expected propeller-like arrangement of the three phenyl rings in both **1** and **2**. The average planes encompassing the three phenyl rings in the two complexes are roughly orthogonal, showing a mean value of 77°. The average P–C_{ipso} bond length is 1.813 Å, and this compares quite well with the mean (1.816 Å) for nearly 1600 monodentate –PPh_3 ligands bound to a gold centre in the CCDC database.

The CCDC repository was also inspected for mononuclear 2-coordinate (N, P) gold complexes in which the nitrogen and the phosphorous atoms belong, respectively, to a penta-atomic ring and to a triphenylphosphane ligand. This search returned only a tenth of the entries from few research groups.[20,27,29,43–48] In these structures, the ranges for the Au–P, Au–N distances are 2.229–2.243 and 1.971–2.077 Å, respectively. Bond lengths in the present work fit within these ranges except for the Au–P length in **2** (see Table 3), which is just a little bit shorter (2.224 (2) Å). Among known structures, those showing more similarity to **1** and **2** (that is, showing exactly a pyrazolate (1-) and a triphenylphosphane ligand) are those with the CCDC codes LAHMAJ,[20] namely 3,5-bis-[(4-octyloxy)phenyl]-1H-pyrazolate)(triphenylphosphine)gold and QESRUB,[27] [(triphenylphosphine)-(pyrazolyl)–gold(I)]; however, the structures found in this work with the codes WULFIT[43] are the ones that better resemble the Au–P, Au–N bonds and they were [(1H-benzotriazol-1-yl)-triphenylphosphine–gold(I)], and MALRIA,[47] [tetrazolyl-triphenylphosphine–gold(I)] (with **1**-I), which also shows a negatively charged nitrogen ligand, and OBIVUR[48] [(3,5-bis(4-n-butoxyphenyl)pyrazole-*N*)-(triphenylphosphine)–gold(I)p-toluenesulfonate] (with **1**-II).

The examination of the packing diagram did not reveal any classic hydrogen bonds for either of the complexes. In **2**, an inspection of the shortest non-bonding contacts showed that the O(2) and O(3) atoms of one molecule loosely (O–H > 2.50 Å) interact, respectively, with the hydrogen atoms bonded to the C (5) and C(14) of a nearby molecule. The motif develops along the crystallographic b axis and appears to be a consequence of π–π stacking effects. The molecules of **2** are piled along the same axis in a head-to-tail arrangement so that the pyrazolate ligand of one molecule faces a second pyrazolate on one side. On the other side, it faces the phenyl ring of the PPh_3 moiety, which is almost coplanar with it. The distance between the centroids of the facing pyrazolate ligands is 3.50 Å, and 3.86 Å between the pyrazolate and the phenyl rings (compared with 3.40 Å in graphite).

In **1**, the shortest non-bonding contacts are those coupling molecules I and II *via* the N(3) and N(4) atoms if the disordered

Table 3 Selected bond lengths (Å) and angles (°) for complexes (**2**) and (**1**). The column for **1** reports the parameters for the two independent molecules (I and II) within the asymmetric unit

2		**1**			
		Molecule I		*Molecule II*	
Au–P	2.224 (2)	Au(1)–P(1)	2.239 (1)	Au(2)–P(2)	2.243 (2)
Au–N(1)	2.065 (5)	Au(1)–N(1)	2.048 (5)	Au(2)–N(2)	2.058 (5)
N(1)–N(2)	1.339 (7)	N(1)–N(3)	1.340 (7)	N(2)–N(4)	1.356 (6)
N(1)–C(3)	1.339 (8)	N(1)–C(1)	1.356 (7)	N(2)–C(24)	1.340 (8)
P–C_{Ph}[a]	1.810	P–C_{Ph}[a]	1.818	P–C_{Ph}[a]	1.811
P–Au–N(1)	174.5 (2)	P(1)–Au(1)–N(1)	178.0 (1)	P(2)–Au(2)–N(2)	175.1 (1)
Au–P–C(4)	110.9 (2)	Au(1)–P(1)–C(6)	113.1 (2)	Au(2)–P(2)–C(29)	111.7 (2)
Au–P–C(10)	111.0 (2)	Au(1)–P(1)–C(12)	111.6 (2)	Au(2)–P(2)–C(35)	109.4 (2)
Au–P–C(16)	115.9 (2)	Au(1)–P(1)–C(18)	113.2 (2)	Au(2)–P(2)–C(41)	114.8 (2)
Au–N(1)–N(2)	122.1 (4)	Au(1)–N(1)–N(3)	118.8 (4)	Au(2)–N(2)–N(4)	121.3 (4)
Au–N(1)–C(3)	128.8 (4)	Au(1)–N(1)–C(1)	131.7 (4)	Au(2)–N(2)–C(24)	127.5 (4)

[a] Mean of three values.

CF_3 residue is not considered. The latter are, again, loosely connected (N–H > 2.48 Å) with the hydrogen atoms bonded to the C(9) and C(46) of a proximal molecule. Contrary to **2** above, however, these contacts do not originate π–π stacking motifs.

Biological studies

The antiproliferative effects of gold(I) azolate compounds were investigated in a panel of various human cancer cells containing samples of breast (MCF-7), lung (A549), cervical (A431), colon (LoVo and LoVo MDR), and ovarian (2008 and C13*) cancers. Cytotoxicity was evaluated by means of an MTT test after 72 h of treatment with increasing concentrations of the tested compounds. For comparison purposes, the cytotoxicity of cis-platin, the most widely used metallodrug, was evaluated in the same experimental conditions. The IC_{50} values, calculated from dose-survival curves, have been reported in Table 4. Uncoordinated azole ligands proved to be scarcely effective in decreasing cancer cell viability over 7 cell lines. Compound **4** was not tested for its cytotoxicity owing to the poor solubility in DMSO and in other solvents suitable for biological testing. Among the gold(I) coordination compounds, triphenylphosphane derivatives proved to be more effective with respect to the TPA analogues. The TPA derivatives **3**, **6** and **8** showed mean IC_{50} (μM) values (excluding those calculated for LoVo MDR and C13*cells) of 32.81 (27.11–43.44), 17.92 (10.31–24.35) and 12.15 (6.48–17.45), respectively, which were from 2 to 4 times higher than that of cis-platin (7.63 μM). The triphenylphosphane derivatives **5** and **7** showed a relevant antiproliferative activity eliciting IC_{50} values (μM) within the same order of magnitude (average IC_{50} of 1.03 and 1.21 μM for **5** and **7**, respectively) and about 6 times lower than cis-platin. Compound **9**, possessing the C–Au–P environment, despite retaining an antiproliferative activity slightly lower than that of the relative compound **7** with an N–Au–P environment, displayed a cytotoxic potency about 2-fold higher than that of the reference metallodrug cis-platin. Notably, compounds **1** and **2** emerged as the most effective in killing cancer cells, with IC_{50} averages roughly 10 times lower than those of cis-platin (average IC_{50} of 0.89 and 0.68 μM for **1** and **2**, respectively). Interestingly, these complexes reached anti-tumor activities in the low micromolar range, which were even lower than those obtained with the phosphine gold(I) drug auranofin.[38,48]

With all the azolate gold(I) complexes, very interesting results have been obtained against the ovarian carcinoma cis-platin-resistant (C13*) cells. In C13* cells, cis-platin resistance has been correlated with reduced cell drug uptake, high cellular TrxR and glutathione levels, and enhanced repair of DNA damage.[49] Cytotoxicity assays testing all the gold(I) derivatives **1–9** against the 2008/C13* cell line pair showed a similar pattern of response across the parental and resistant sub-lines and allowed the calculation of RF values (RF = Resistant Factor, which is defined as the ratio between IC_{50} values calculated for the resistant cells and those arising from the sensitive ones) roughly 7.5-fold lower than that obtained with cis-platin (RF = 9.0) (see Table 4). These data clearly reveal no cross-resistance phenomena.

Additionally, gold(I) complexes were tested against a multi-drug resistant (MDR) colon carcinoma subline, LoVo MDR cells. It is well known that acquired MDR, whereby cells become refractory to multiple drugs, represents a major barrier to the success of chemotherapy. Although most metal complexes are not P-glycoprotein substrates, several multidrug resistance proteins (MRP1, MRP2, MRP4) have been found to be involved in Pt uptake and are responsible for its efflux/afflux from cells.[49–51] The resistance of LoVo MDR cells to doxorubicin, a drug belonging to the MDR spectrum, is associated with an overexpression of the multi-specific drug transporters, such as, for example, the 170 kDa P-glycoprotein (P-gp).[52] Tested on a LoVo/LoVo MDR cell line pair, pyrazolategold(I)-triphenylphosphane and -TPA derivatives allow the calculation of an RF value up to 10 times lower than that obtained with doxorubicin, clearly suggesting that pyrazolategold(I) complexes are not potential MDR substrates. Conversely, 4,5-dichloro-1-imidazolate–gold(I) derivatives **7** and **8** showed a significantly lower cytotoxicity potency against resistant sub-line LoVo MDR, attesting they do not overcome MDR phenomena.

Table 4 *In vitro* antitumor activity

Compound	IC_{50} (μM) ± S.D. MCF-7	A549	A431	LoVo	LoVo MDR	R.F.	2008	C13*	R.F.
$PPh_3Au(3,5\text{-}pz^{CF3})$ **1**	1.03 ± 0.59	0.96 ± 0.34	0.63 ± 0.31	0.90 ± 0.52	1.49 ± 2.54	1.7	0.91 ± 1.01	0.72 ± 0.19	0.8
$PPh_3Au(3,5\text{-}pz^{NO2})$ **2**	0.53 ± 0.35	0.49 ± 0.21	0.82 ± 0.40	0.73 ± 0.30	1.23 ± 0.95	1.7	0.81 ± 0.32	0.52 ± 0.22	0.8
$TPAAu(3,5\text{-}pz^{CF3})$ **3**	43.44 ± 2.15	32.93 ± 2.38	29.47 ± 1.22	31.12 ± 3.42	54.81 ± 2.12	1.7	27.11 ± 2.31	33.36 ± 1.18	1.2
$TPAAu(3,5\text{-}pz^{NO2})$ **4**	ND	ND	ND	ND	ND	—	ND	ND	—
$PPh_3Au(4\text{-}pz^{NO2})$ **5**	1.62 ± 0.97	1.03 ± 0.25	0.51 ± 0.21	0.86 ± 0.67	0.98 ± 1.21	1.1	1.12 ± 1.33	2.01 ± 1.18	1.9
$TPAAu(4\text{-}pz^{NO2})$ **6**	24.35 ± 2.35	23.24 ± 2.31	15.32 ± 1.54	10.13 ± 0.91	17.12 ± 3.35	1.7	16.54 ± 3.96	27.75 ± 3.01	1.7
$PPh_3Au(4,5\text{-}im^{Cl})$ **7**	1.13 ± 0.74	3.05 ± 1.52	1.13 ± 0.49	1.05 ± 0.34	9.58 ± 1.34	9.1	2.17 ± 0.87	1.21 ± 0.94	0.6
$TPAAu(4,5\text{-}im^{Cl})$ **8**	13.63 ± 2.08	17.45 ± 2.11	7.45 ± 1.05	6.48 ± 1.27	26.96 ± 3.51	4.1	15.76 ± 1.73	9.45 ± 1.93	0.6
$PPh_3Au(4,5\text{-}im^{1\text{-}Bz,Cl})$ **9**	4.16 ± 0.97	3.99 ± 1.25	1.98 ± 0.52	3.19 ± 0.74	6.66 ± 1.02	2.0	3.78 ± 1.21	4.04 ± 1.12	1.7
$3,5\text{-}pz^{CF3}$	61.63 ± 2.62	38.61 ± 2.20	49.92 ± 2.27	41.13 ± 3.42	53.21 ± 3.47	1.3	39.97 ± 1.11	51.55 ± 2.24	1.3
$3,5\text{-}pz^{NO2}$	45.63 ± 0.93	44.49 ± 0.91	38.24 ± 2.55	30.34 ± 1.77	54.87 ± 2.96	1.8	33.38 ± 1.13	58.63 ± 3.14	1.7
$4\text{-}pz^{NO2}$	>100	>100	>100	>100	>100	—	>100	>100	—
$4,5\text{-}Im^{Cl}$	67.12 ± 1.64	56.72 ± 1.54	52.51 ± 1.83	51.12 ± 1.32	>100	—	60.34 ± 3.04	44.52 ± 1.24	—
cis-platin (doxorubicin)	10.31 ± 1.36	13.42 ± 1.96	2.08 ± 1.06	8.03 ± 1.23 (1.11 ± 0.86)	8.51 ± 1.37 (19.21 ± 2.37)	1.1 (17.3)	4.35 ± 1.59	39.34 ± 2.92	9.0

S.D. = standard deviation. IC_{50} values were calculated by four parameter logistic model ($P < 0.05$). Cells ($3–8 \times 10^4$ mL^{-1}) were treated for 72 h with increasing concentrations of tested compounds. Cytotoxicity was assessed by MTT test. R.F. (resistance factor) = IC_{50} resistant cells/IC_{50} sensitive cells.

Table 5 *In vitro* inhibition of purified TrxR and GR

Compound	TrxR1 IC_{50} (nM)	TrxR2 IC_{50} (nM)	GR IC_{50} (μM)
1	3.50	38.12	1.96
2	15.80	48.12	1.78
5	86.54	258.30	0.08
7	7.14	33.57	0.13

S.D. = standard deviation. TrxR1 and TrxR2 activity was assessed by measuring NADPH-dependent reduction of DTNB at 412 nm; GR activity was followed at 340 nm. IC_{50} values were calculated by four parameter logistic model ($P < 0.05$).

In vitro inhibition of purified TrxR and GR

Based on the cytotoxicity test results, gold(I)-triphenylphosphane derivatives (**1**, **2**, **5** and **7**) were selected for further molecular pharmacological studies. In reality, as the selenoenzyme TrxR has been generally recognized as the most relevant molecular target for gold complexes,[53] the ability of the azole gold(I)-triphenylphosphane complexes to inhibit TrxR activity has been evaluated. Moreover, their inhibitory activity towards disulfide reductase GR, which is structurally closely related to TrxR, has been assessed.

The inhibitory effects of gold(I) complexes on rat isolated cytosolic (TrxR1) or mitochondrial (TrxR2) isoforms of TrxR were measured according to standard procedures.[54] Gold(I) complexes were tested at increasing concentrations and IC_{50} values were calculated from the dose-effect curves (Table 5). The cytosolic isoform appeared markedly inhibited by **1**, **2** and **7** derivatives at nanomolar concentrations (IC_{50} of 15.8 nM, 3.5 nM and 7.14 for **1**, **2** and **7**, respectively). On the other hand, higher concentrations were required for a reduction of 50% of TrxR2 activity for all the derivatives compared with TrxR1 (Table 5). This difference in sensitivity had been previously underlined for many other gold(I) complexes, including auranofin and other phosphine gold(I) complexes,[55] and may be consistent with the different sequence of the two TrxR isoforms and the greater acidity of TrxR1.[56]

Tested against GR, compounds **5** and **7** revealed a significant ability in inhibiting GR (IC_{50} of 0.8 and 0.13 μM for **5** and **7**, respectively). Differently, **1** and **2** proved to have a lower effect with IC_{50} values in the micromolar range, one order of magnitude higher than those detected for TrxR isoforms. This result clearly attests a significant selectivity for TrxR inhibition over GR inhibition, similarly to data previously obtained with other phosphane gold derivatives.[55,56]

Inhibition of redox enzymes in human ovarian cancer cells

TrxR and GR inhibition were also evaluated in 2008 cells treated for 12 h with IC_{50} concentrations of gold(I)-triphenylphosphane derivatives. TrxR activity was assayed by measuring at 412 nm NADPH-dependent reduction of DTNB (Fig. 2, panel A) as well as TrxR-mediated insulin reduction (Fig. 2 panel A, insert a). Compounds **5** and **7** decreased TrxR activity by roughly 60% whereas **1** and **2** were found to be able to decrease cellular TrxR activity by approximately 85% with respect to untreated cells. Conversely, disulfide isomerase GR was less intensely inhibited by these gold(I) complexes (Fig. 2, panel B and C). The tested compounds were also evaluated as potential inhibitors of GPx, a different Sec-containing redox enzyme. Interestingly, none of the tested complexes caused a significant decrease in GPx activity, attesting the gold(I)-triphenylphosphane derivative selectivity towards the TrxR enzyme. This difference shown by gold(I) derivatives in the inhibitory potencies of TrxR and GPx may be correlated with Sec accessibility in the selenoenzyme active sites. Indeed, unlike the flexible C-terminus active site of TrxR, the active site of GPx is located at the N-terminal end of α-helices, surrounded by aromatic side chains.[57] That context may protect Sec from a gold(I) electrophilic attack.

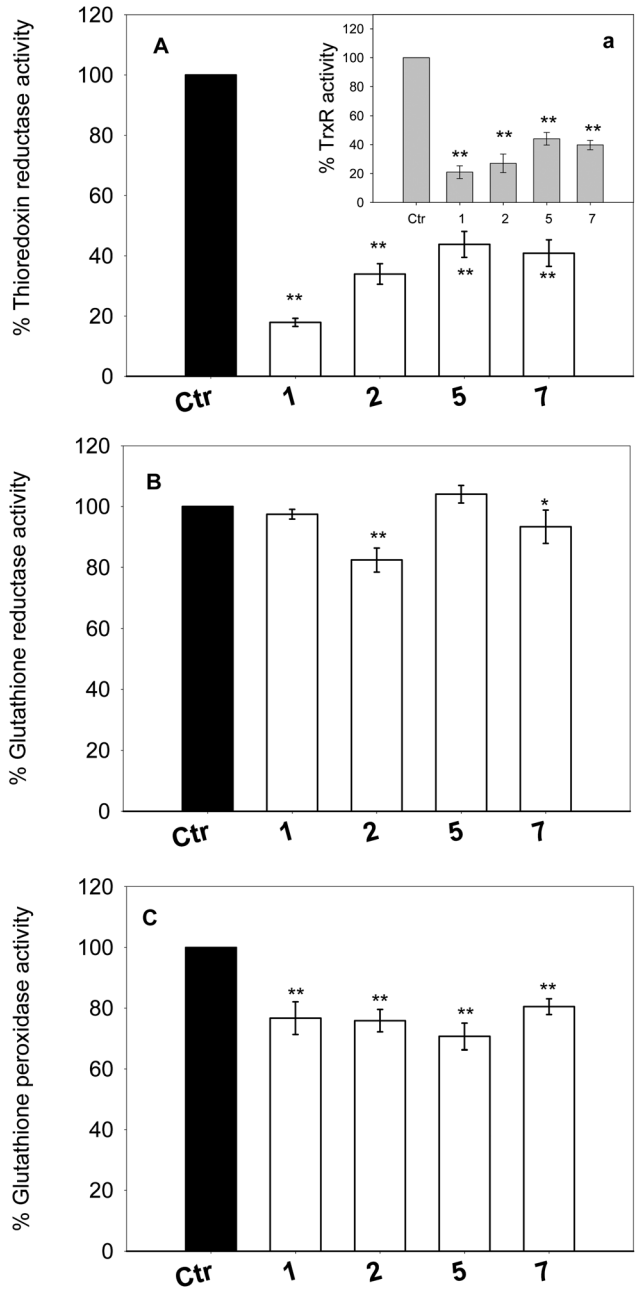

Fig. 2 Effects of gold(I)–triphenylphosphane compounds on redox enzymes in human ovarian cancer cells. 2008 cells were incubated for 12 hours with IC_{50} of tested compounds. Subsequently, cells were washed twice with PBS and lysed. TrxR activity was tested by measuring NADPH-dependent reduction of DTNB (A) and by insulin reduction assay (insert a) at 412 nm; GR activity (B) and GPx (C) activities were followed at 340 nm. All the values are the means ± SD of not less than three measurements. Multiple comparisons were made by the one-way analysis of variance followed by the Tukey–Kramer multiple comparison test or ANOVA test (**$p < 0.01$; *$p < 0.05$).

Conclusions

The synthesis of nine new neutral azolate gold(I) phosphane compounds has been performed with medium to good yields. The use of pyrazoles substituted with deactivating groups in the 3- and 5- or 4-position and that of imidazole with chlorides in the 4- and 5-position in addition to the use of phosphane ligands with different cone angle (PPh_3 = 145° and TPA = 102°), gave mononuclear derivatives as the main product. The introduction of deactivating groups in the azolate rings had a double function. The first aim was to avoid the typical cyclization resulting in nine-membered cycles or polynuclear derivatives and the second was to get a better solubility in polar solvents. Moreover, for the latter scope, a more polar phosphane co-ligand as the TPA has been employed too. However, in the biological tests, triphenylphosphane derivatives possess better *in vitro* antitumor properties compared with the TPA analogues. By increasing the deactivation potency of the substituents on the pyrazole ring an increase of the antiproliferative activity has been achieved (**2** > **1** > **5**) among the pyrazolate gold(I)-triphenylphosphane series. Complexes **1** and **2** were tested for their ability to inhibit cytosolic and mitochondrial TrxR *in vitro* and they were found to efficiently hamper enzyme activity at concentrations that did not affect the related oxidoreductase GR. Moreover, in 2008 human ovarian cancer cells, the scarce effect in inactivating the flavoenzymes GR and the Sec-containing enzyme GPx revealed for **1** and **2** a certain selectivity towards TrxR.

Experimental section

Synthesis

Elemental analyses (C, H, N, and S) were performed in-house with a Fisons Instruments 1108 CHNS-O Elemental Analyser. Melting points were taken on an SMP3 Stuart Scientific Instrument. IR spectra were recorded from 4000 to 600 cm^{-1} with a Perkin-Elmer SPECTRUM ONE System FT-IR instrument. IR annotations used: br = broad, m = medium, mbr = medium broad, s = strong, sh = shoulder, vs = very strong, w = weak and vw = very weak. ^1H and ^{31}P NMR spectra were recorded on an Oxford-400 Varian spectrometer (400.4 MHz for ^1H and 162.1 MHz for ^{31}P). Chemical shifts, in ppm, for ^1H NMR spectra are relative to internal Me_4Si. ^{31}P NMR chemical shifts were referenced to a 85% H_3PO_4 standard. The ^{31}P NMR spectroscopic data were accumulated with ^1H decoupling. NMR annotations used: br = broad, d = doublet, m = multiplet, s = singlet. Electrospray mass spectra (ESI-MS) were obtained in positive- or negative-ion mode on a Series 1100 MSD detector HP spectrometer (1100 Series MSD detector), using an acetonitrile or methanol mobile phase. The compounds were added to the reagent grade acetonitrile to give solutions of approximate concentration 0.1 mM. These solutions were injected (1 µl) into the spectrometer *via* a HPLC HP 1090 Series II fitted with an autosampler. The pump delivered the solutions to the mass spectrometer source at a flow rate of 300 µl min^{-1}, and nitrogen was employed both as a drying and nebulizing gas. Capillary voltages were typically 4000 V and 3500 V for the positive- and negative-ion mode, respectively. Confirmation of all major species in this ESI-MS study was aided by comparison of the observed and predicted isotope distribution patterns, the latter calculated using the IsoPro 3.0 computer program. The used solvents were HPLC grade and they were used as purchased, unless water and oxygen sensitive reactions were led. In this last case anhydrous and radicals free THF was obtained by treating the solvent with Na/acetophenone under a N_2 atmosphere.

Materials

3,5-bis(trifluoromethyl)pyrazole and other chemicals were purchased and used without further purification. The complex Ph_3PAuCl was synthesized from tetrachloridegold(I) acid and a double molar amount of PPh_3 in ethyl alcohol as previously reported.[58] The synthesis of the 3,5-dinitropyrazolate ligand was performed as previously reported in literature,[59] only the purification was led with a slight modification to obtain the pure sodium salt. In fact, after the second pyrolysis, the mixture of 3,5-dinitropyrazole and 3-nitropyrazole was treated with NaOH 1M. The resulting salts were then acidified by glacial CH_3COOH until pH 5 to protonate only the 3-nitropyrazole. The pure sodium 3,5-dinitropyrazolate was extracted with hot benzene and obtained as a solid with a yield of more than 70%.

Synthesis of [(3,5-bis-trifluoromethyl-1H-pyrazolate-1-yl)-triphenylphosphane–gold(I)] (1). To a solution of CH_3OH (6 mL) and 3,5-bis(trifluoromethyl)pyrazole (0.1 g, 0.49 mmol), 2.75 mL of 1% methanolic solution of KOH (0.49 mmol) was added. After a few minutes, 5 mL of a solution of Ph_3PAuBF_4 in THF (0.49 mmol) was added. After magnetic stirring of an hour, the suspension was filtered. The colorless solution was then concentrated to dryness under vacuum and an oily product was obtained. The crude product was washed with hexane and crystallized by a mixture of CH_2Cl_2–hexane. Yield 75%. M. p. 124.2–125.8 °C. ^{1}H NMR (CD_2Cl_2, 293 K): δ 7.62–7.56 (m, 15H, PPh_3), 6.96 (s, 1H, pz). ^{31}P NMR (CD_2Cl_2, 293 K): δ 31.79 (s). IR (cm^{-1}): 3144vw (C-Hpz), 3059vw, 3048vw, 1621vw, 1589w, 1546m, 1530m, 1497m, 1482m, 1436s (NO_2), 1352m, 1332w, 1310w, 1253vs (NO_2), 1220s, 1157s sh, 1139vs, 1101vs, 1075s, 1010vs, 974s, 925m, 849m, 816m, 745s, 712s, 689vs. ESI(+) (CH_3CN) *m/z* %: 242.3 (18) $[3,5(CF_3)_2pz + K]^+$, 500.1 (30) $[Au(PPh_3) + CH_3CN]^+$, 721.3 (25) $[Au(PPh_3)_2]^+$, 1121 (100) $[Au(PPh_3)_2 + 3,5(CF_3)_2pzAu]^+$; ESI(−) ($CH_3CN$) *m/z*, %: 202.9 (70) $[3,5\text{-}(CF_3)_2pz)]^-$, 468.5 (55), 602.3 (100) $[3,5(CF_3)_2pz)_2Au]^-$. Elemental analysis for $C_{23}H_{16}AuF_6N_2P$, calcd %: C, 41.71; H, 2.43; N, 4.23. Found %: C, 41.82; H, 2.17; N, 4.54.

Synthesis of [(3,5-dinitro-1H-pyrazolate-1-yl)-triphenylphosphane–gold(I)] (2). Solid Ph_3PAuCl (0.494 g, 1 mmol) was dissolved in 10 mL of THF. To this solution solid $AgBF_4$ (0.194 g, 1 mmol) was added. The suspension was stirred for 10 minutes and sodium 3,5-dinitropyrazolate was then added (0.180 g, 1 mmol). The pale yellow suspension was stirred for another hour. After filtration the solution was concentrated to dryness under vacuum to obtain a pale yellow solid. The crude product was washed with water to eliminate salts and the unreacted pyrazolate. The crystallization of the crude solid was performed by dissolving the solid in THF and by layering hexane. Yield 90%. M. p. 162.4–163.5 °C with decomposition. ^{1}H NMR (acetone-d^6, 293 K): δ 7.82–7.60 (m, 16H, PPh_3 + pz), 3.63 (m, 2H, THF), 1.79 (m, 2H, THF). ^{31}P NMR (acetone-d^6, 293 K): δ 31.06 (s). IR (cm^{-1}): 3168vw (C-Hpz), 3054vw, 3030vw, 1677w, 1585w, 1543s, 1489vs, 1449s, 1435vs, 1361vs, 1325vs, 1294s, 1181s, 1098vs, 1067m, 1046m, 1025m, 995m, 923w, 831s, 812s, 740vs, 711s, 679vs. ESI (+) (CH_3CN) *m/z* %: 500.3 (37) $[AuPPh_3 + CH_3CN]^+$, 721.3 (100) $[Au(PPh_3)_2]^+$, 935 (10), 1075.3 (30) $[Au(PPh_3)_2 + 3,5(NO_2)_2pzAu]^+$; ESI (−) ($CH_3CN$) *m/z* %: 156.9 (100) $[3,5\text{-}(NO_2)_2pz]^-$, 376.6 (30). Elemental analysis for $C_{21}H_{16}AuN_4O_4P \cdot 0.5THF$, calcd %: C, 42.35; H, 3.09, N, 8.59. Found %: C, 42.50; H, 3.09; N, 8.40.

Synthesis of [(3,5-bis-trifluoromethyl-1H-pyrazolate-1-yl)-(1,3-5-triaza-phosphaadamantane)–gold(I)] (3). To a CH_3CN solution (6 mL) of 3,5-bis(trifluoromethyl)pyrazole (0.031 g, 0.15 mmol), 0.85 mL of 1% methanolic solution of KOH (0.15 mmol) was added. To this solution, 1,3-5-triaza-phosphaadamantanegold(I)chloride (0.060 mg, 0.157 mmol) dissolved in 30 mL of CH_3CN was added. The mixture reaction was stirred for two hours at room temperature and for an hour at 40 °C. After filtration, the solution was concentrated to dryness under vacuum to obtain a pale yellow solid. The crude product was then dissolved in CH_2Cl_2 (10 mL) and washed with water (3 × 5 mL). The dichloromethane solution was then dried over a bed of anhydrous Na_2SO_4 and evaporated to dryness to obtain a white solid (65 mg) in 75% of yield. M. p. 200.1–202.3 °C. ^{1}H-NMR (acetone-d^6, 293 K): δ 6.99 (s, 1H, pz), 4.74 (d, 6H, $^2J_{P\text{-}H}$ = 12.8 Hz, PCH_2N), 4.58 (s, 4H, NCH_2N_{eq}), 4.54 (s, 2H, NCH_2N_{ax}). ^{31}P{^{1}H} NMR (acetone-d^6, 293 K): δ −57.94 (s). IR (cm^{-1}): 3109w (C-Hpz), 3060w, 2952w, 2916w, 2867m, 1711m, 1672m, 1546m, 1497sh, 1438m, 1417m, 1411m, 1362m, 1338m, 1257vs, 1243vs, 1217vs, 1155m, 1108vs, 1094vs, 1040m, 1009vs, 972vs, 964vs, 945vs, 900m, 854m, 807vs, 752m, 738vs, 718m. ESI(+) (CH_3OH), *m/z* (%): 242.3 (100) $[3,5(CF_3)_2pz + K]^+$. ESI(−) (CH_3OH), *m/z* (%): 602.8 (100) $[(3,5(CF_3)_2pz)_2 + Au]^-$. Elemental analysis for $C_{11}H_{13}AuF_6N_5P$, calcd %: C, 23.71; H, 2.35; N, 12.57. Found %: C, 24.30; H, 2.28, N, 12.35.

Synthesis of [(3,5-bis-dinitro-1H-pyrazolate-1-yl)-(1,3-5-triaza-phosphaadamantane)–gold(I)] (4). To an aqueous methanol solution (20 mL of CH_3OH and 1 mL of H_2O) of sodium 3,5-dinitropyrazolate (0.046 g, 0.25 mmol), solid 1,3-5-triaza-phosphaadamantanegold(I)chloride (0.100 g, 0.25 mmol) was added. A lemon yellow precipitate was readily obtained. The mixture reaction was stirred overnight. After filtration over a paper filter a yellow solid was collected. The crude product showed scarce solubility in most common solvents and it was purified by washing with water (2 mL × 5 times) and further drying under vacuum (0.101 g). Yield 76%. M. p. 213.1–214.8 °C with decomposition. IR (cm^{-1}): 3149m (C-Hpz), 2949m, 2911m, 2880m, 1547s, 1532m (NO_2), 1490s, 1449m, 1418m, 1354s, 1321s, 1286m (NO_2), 1246m, 1184m, 1097m, 1078m, 1043m, 1014s, 995m, 973vs, 946vs, 907m, 900m, 832m, 815m, 801m, 737vs. Elemental analysis for $C_9H_{13}AuN_7O_4P \cdot CH_3OH \cdot NaCl$, calcd %: C, 19.96; H, 2.85; N, 16.30. Found %: C, 20.66; H, 2.67, N, 16.56.

Synthesis of [(4-nitro-1H-pyrazolate-1-yl)-triphenylphosphane–gold(I)] (5). To a THF solution (8 mL) of 4-nitropyrazole (100 mg, 1.13 mmol) solid NaH (0.0027 g, 1.13 mmol) was added. To this suspension solid triphenylphosphanegold(I) chloride (0.558 g, 1.13 mmol) was added. The suspension was filtered after two hours of stirring. After filtration, the solution was concentrated to dryness under vacuum and a white solid was obtained. After dissolution in CH_2Cl_2, extractions with water (3 × 5 mL) were performed to remove the excess of nitropyrazole

and sodium chloride. The organic phase was dried by anhydrous Na_2SO_4 and evaporated to dryness to obtain the product as a white solid (217 mg) in 55% yield. M. p. 170.8–172.1 °C with decomposition. ^{1}H-NMR (acetone-d^6, 293 K): δ 8.31 (s, 2H), 7.71–7.61 (m, 15H, PPh_3). $^{31}P\{^1H\}$ NMR (acetone-d^6, 293 K): δ 32.12 (s). IR (cm^{-1}): 3119w (C-Hpz), 3075w, 3053w, 2958m, 2924w, 2856m, 1586w, 1549w, 1495s (NO_2), 1479s, 1435s, 1400s, 1331m, 1311m, 1272vs (NO_2), 1157m, 1100m, 1064m, 1023m, 997s, 943m, 860m, 812s, 744vs, 710s, 689vs. ESI(+) (CH_3CN), *m/z* (%): 721 (100) $[Au(PPh_3)_2]^+$. ESI(−) (CH_3CN), *m/z* (%): 112.1 (20) $[4\text{-}NO_2pz]^-$, 180 (100) $[4\text{-}NO_2pzH + 4\text{-}NO_2pz]^-$. Elemental analysis for $C_{21}H_{17}AuN_3O_2P$, calcd %: C, 44.15; H, 3.00; N, 7.35. Found %: C, 44.38; H, 3.09, N, 6.29.

Synthesis of [(4-nitro-1H-pyrazolate-1-yl)-(1,3-5-triaza-phosphaadamantane)–gold(I)] (6). To a THF solution (5 mL) of 4-nitropyrazole (17.7 mg, 0.157 mmol) solid NaH (5.6 mg, 0.235 mmol) was added. After observation of gas evolution and magnetic stirring for half an hour, the suspension was filtered over a celite bed (1.5 cm) and dropped into a solution of 1,3-5-triaza-phosphaadamantanegold(I)chloride (0.060 g; 0.157 mmol) dissolved in 30 mL of CH_3CN. The pale white suspension was stirred for an hour at room temperature and another hour at 40 °C. After filtration, the solution was concentrated to dryness under vacuum and a solid white was obtained. After dissolution in CH_2Cl_2, extractions with water (3 × 5 mL) were performed to remove the excess of nitropyrazole and sodium chloride. The organic phase was then dried over a bed of anhydrous Na_2SO_4 and evaporated to dryness to obtain the product as a white solid (43 mg) in 59% yield. M. p. 203.2–204.8 °C with decomposition. ^{1}H-NMR (DMSO, 293 K): δ 8.34 (s, 2H), 4.49 (d, 6H, $^2J_{P\text{-}H}$ = 16 Hz, PCH_2N), 4.35 (s, 2H, NCH_2N_{ax}), 4.33 (s, 4H, NCH_2N_{eq}). $^{31}P\{^1H\}$ NMR (DMSO, 293 K): δ −52.52 (s). IR (cm^{-1}): 3138w (C-Hpz), 2922m, 2853m, 1551m, 1496s (NO_2), 1444w, 1405s, 1358m, 1333m, 1275vs (NO_2), 1242vs, 1162m, 1100m, 1040m, 1011vs, 969vs, 946vs, 900m, 813m, 801 vs, 752m, 733vs. ESI(+) (CH_3CN), *m/z* (%): 242.4 (100). ESI(−) (CH_3CN), *m/z* (%): 112.1 (100) $[4\text{-}NO_2pz]^-$, 420.8 (25) $[Au(4\text{-}NO_2pz)_2]^-$. Elemental analysis for $C_9H_{14}AuN_6O_2P$, calcd %: C, 23.19; H, 3.03; N, 18.03. Found %: C, 22.89; H, 2.72; N, 17.31.

Synthesis of [(4,5-dichloro-1H-imidazolate-1-yl)-triphenylphosphane–gold(I)] (7). 50 mgs (0.36 mmol) of 4,5-dichloroimidazole were dissolved in 10 mL of CH_3OH. To this solution 0.36 mL of methanolic NaOH 1 M were added (0.36 mmol). After stirring for 15 min, 179 mg of solid PPh_3AuCl (0.36 mmol) were added. The solution was stirred for four hours. After filtering on paper the solution was concentrated to dryness under vacuum obtaining a white solid. The crude product was washed with hexane (2 × 3 mL), pumped to dryness and then with water (2 × 5 mL) to eliminate salts and the unreacted imidazolate. The compound was dried by vacuum (182 mg). Yield 84%. M.p. 155.2–156.8 °C with decomposition. ^{1}H-NMR (acetone-d^6, 293 K): δ 7.72–7.62 (m, 15H, PPh_3), 7.16 (s, 1H, Im), 2.87 (s, br, 2H, H_2O). ^{31}P NMR (acetone-d^6, 293 K): δ 32.34 (s). IR (cm^{-1}): 3150w (C-Him), 3054w, 3032w, 1587m, 1499m, 1480m, 1434s, 1331m, 1309m, 1259m, 1222s, 1188m, 1101s, 1041m, 1011s, 997m, 963m, 920m, 812m, 743s, 711s, 689vs. ESI(+) (CH_3CN), *m/z* (%): 1053.1 (100) $[Au(PPh_3)_2 + 4,5\text{-}Cl_2Im]^+$. ESI(−) ($CH_3CN$), *m/z* (%): 134.9 (100) $[4,5\text{-}Cl_2Im]^-$, 468.9 (40) $[Au(4,5\text{-}Cl\text{-}Im)_2]^-$. Elemental analysis for $C_{21}H_{16}AuCl_2N_2P \cdot H_2O$, calcd %: C, 41.13, H, 2.96, N, 4.57. Found %: C, 41.25, H, 2.64, N, 4.91.

Synthesis of [(4,5-dichloro-1H-imidazolate-1-yl)-(1,3-5-triaza-phosphaadamantane)–gold(I)] (8). 40 mg of 4,5-dichloroimidazole (0.29 mmol) were dissolved in 10 mL of CH_3OH. To this solution 0.29 mL of a 1 M methanolic solution of NaOH (0.29 mmol) was added. After stirring for 10 minutes, solid TPAAuCl (0.113 g, 0.29 mmol) was also added. A white precipitate was readily formed and the suspension was stirred at room temperature for 5 h. The suspension was filtered off through a paper filter. The white solid was washed with water (4 × 3 mL) and dried by vacuum (112 mg). Yield: 78%. M.p. >250 °C with decomposition starting from 200 °C. ^{1}H-NMR (DMSO, 293 K): δ 7.00 (s, 1H, Im), 4.51 (d, 6H, $^2J_{P\text{-}H}$ = 12 Hz, PCH_2N), 4.37 (s, 2H, NCH_2N_{ax}), 4.30 (s, 4H, NCH_2N_{eq}). $^{31}P\{^1H\}$ NMR (DMSO, 293 K): δ −52.52 (s). IR (cm^{-1}): 3124w (C-Him), 2963m, 2948m, 2927m, 2833m, 1652m, 1493m, 1466m, 1439s, 1427m, 1411m, 1284s, 1241s, 1228vs, 1190s, 1099m, 1040m, 1010s, 967vs, 945vs, 901m, 824m, 801s, 738s, 668m. Elemental analysis for $C_9H_{13}AuCl_2N_5P$, calcd %: C, 22.06, H, 2.67, N, 14.29. Found %: C, 22.25, H, 2.62, N, 13.90.

Synthesis of [(1-benzyl-4,5-dichloro-2H-imidazolate-2-yl)-triphenylphosphane–gold(I)] (9)

Synthesis of 1-benzyl-4,5-dichloroimidazole. 700 mg of 4,5-dichloroimidazole (5.1 mmol) were dissolved in 10 mL of DMF. To this solution 0.58 mL of benzylchloride (5.1 mmol) and 540 mg of Na_2CO_3 (5.1 mmol) were added. The suspension was stirred at reflux overnight. After filtering on paper the solution was concentrated to dryness under vacuum obtaining an orange oil. The oil was treated with 30 mL of water and stirred vigorously until a solid was formed. The solid was recovered by filtration and dissolved in diethyl ether. The ether solution was first filtered and then concentrated to dryness under vacuum. A pale orange solid was obtained. Yield 65%. M. p. 60.2–61.4 °C. ^{1}H-NMR (acetone-d^6, 293 K): δ 7.81 (s, 1H, C2-H), 7.39–7.28 (m, 5H, C_6H_5), 5.30 (s, 2H, CH_2bz). IR (cm^{-1}): 3124m (C-Him), 3067w, 3033w, 1519m, 1496m, 1456m, 1483m, 1389m, 1364w, 1345m, 1253s, 1215m, 1201w, 1180m, 1114m, 1078m, 975m, 951w, 911w, 854w, 806m, 782m, 717vs, 692vs, 662s. Elemental analysis for $C_{10}H_8Cl_2N_2$, calcd %: C, 52.89, H, 3.55, N, 12.34. Found %: C, 53.21, H, 3.43, N, 12.16.

Synthesis of [(1-benzyl-4,5-dichloro-2H-imidazolate-1-yl)-triphenylphosphane–gold(I)]. 136 mg of the 1-benzyl-4,5-dichloroimidazole (0.6 mmol) were dissolved in 10 mL of anhydrous THF under a nitrogen flux. To this solution 0.24 mL of n-BuLi (0.6 mmol) were added to this solution at −40 °C and the dark orange solution was stirred at this temperature for an hour. The solution was heated to 0 °C and solid PPh_3AuCl was added (0.297 g; 0.6 mmol). The color of the solution readily turned to dark brown and it was stirred for two hours. After this time the solvent was evaporated and the oily residue was treated with CH_2Cl_2 (10 mL). The dichloromethane solution was then treated with water (4 × 10 mL) and collected in a flask and dried over

anhydrous Na_2SO_4. After removal of the solvent the crude product was suspended in hexane and stirred vigorously overnight. The pale brown solid obtained was filtered and dried. The impurities were precipitated by dissolving the crude product in $CHCl_3$ and by layering hexane. After the removal of the solvents 0.182 g of an ivory solid was recovered. Yield 42%. M. p. 152.1–153.6 °C. ^{1}H-NMR ($CDCl_3$, 293 K): δ 7.50–7.38 (m, 15H, PPh_3), 7.25–7.21 (m, 5H, C_6H_5), 5.29 (s, 2H, CH_2bz). ^{31}P NMR ($CDCl_3$, 293 K): δ 43.13 (s). IR (cm^{-1}): 3070w (C-Him), 3047w, 3032w, 2988w, 1586w, 1519m, 1496m, 1481m, 1455m, 1435s, 1398m, 1342m, 1331m, 1310m, 1293m, 1222s, 1193m, 1181m, 1100s, 1075m, 1027m, 998m, 958m, 851m, 749s, 727s, 710s, 691vs. ESI(+) (CH_3CN), *m*/*z* (%): 685.0 (70) [(4,5-Cl_2bzim)AuPPh$_3$ + H]$^+$, 721.2 (100) [Au(PPh_3)$_2$]$^+$, 1108.9 (40) [(4,5-Cl_2bzim)$_2$AuPPh$_3$ + H]$^+$. Elemental analysis for $C_{28}H_{22}AuCl_2N_2P$, calcd %: C, 48.84, H, 3.17, N, 4.07. Found %: C, 49.07, H, 3.24, N, 4.09.

X-Ray analyses

Single crystals of the complexes 3,5-bis(trifluoromethyl)pyrazolategold(I)triphenylphosphane (**1**) and 3,5-bis(dinitro)pyrazolategold(I)triphenylphosphane (**2**) of X-ray quality were grown by slow diffusion of hexane into a solution of CH_2Cl_2 for **1**, and by layering hexane on a THF solution for **2**. Adequate specimens were lodged on glass fibers and centred on the goniometer head of two different instruments, thanks to the generosity of Colleagues from the Chemistry Department of the University of Trieste, Italy (**1**) and of the C.N.R.–I.C.I.S. Institute of Padua, Italy (**2**). The crystal chosen for **1** was mounted on an Enraf-Nonius DIP1030 image plate diffractometer, and the selected specimen for **2** was mounted on a Philips PW1100 diffractometer. The raw data were collected, in both cases, at room temperature, by using graphite–monochromated Mo Kα radiation (λ = 0.71073 Å) and corrected for Lorentz/polarization effects, as well as for absorption. In the case of **2**, the absorption correction was performed by means of ψ-scans,[60] while a cubic fit to sin θ/λ values (24 parameters)[61] was used for **1**. Data were collected with ω-2θ scans (**2**) or φ scans (**1**). In **2**, the unit cell parameters were determined by least-squares refinement of 30 well centred high-angle reflections, and two standard reflections were checked every 150 measurements to ensure for crystal stability. In **1**, unit-cell parameters were determined by least-squares refinement during the whole data collection. In both collections no sign of deterioration was detected. The structures were solved by direct methods, with SIR97[62] (**2**) or SHELXTL NT[63] (**1**) and refined by standard full-matrix least-squares based on F_o^2 with the SHELXL-97[64] and OLEX2[65] programs.

In **1**, two independent molecules (from now on, I and II) make the asymmetric unit. During the refinement of molecule II, some peaks appeared in positions compatible with a second arrangement of one of the trifluoromethyl groups. At the end of the refinement, the involved atoms were modelled as disordered over two sites (F(10), F(11), F(12); F(10A), F(11A), F(12A)). The two positions were refined isotropically, with partial occupancies of 0.52 and 0.48, respectively. With this exception, all non-H atoms of **1** and **2** were allowed to vibrate anisotropically in the last cycles of refinement; H atoms were placed instead in calculated positions and refined as "riding model".

Experiments with human cells

Azolate gold(I) complexes and the corresponding uncoordinated ligands were dissolved in DMSO just before the experiment and a calculated amount of drug solution was added to the growth medium to a final solvent concentration of 0.5%, which had no effect on cell killing. cis-platin was dissolved in a 0.9% NaCl solution just before the experiment. MTT (3-(4,5-dimethylthiazol-2-yl)-2,5-diphenyltetrazolium bromide) and cis-platin were obtained from Sigma Chemical Co, St. Louis, USA.

Cell cultures

Human breast (MCF-7) and lung (A549) carcinoma cell lines were obtained from American Type Culture Collection (ATCC, Rockville, MD). A431 human cervical carcinoma cells were kindly provided by Prof. F. Zunino (Division of Experimental Oncology B, Istituto Nazionale dei Tumori, Milan, Italy). 2008 cells and their cis-platin resistant variant, called C13* cells, are human ovarian cancer cell lines, and they were kindly provided by Prof. G. Marverti (Department of Biomedical Science of Modena University, Italy). The LoVo human colon-carcinoma cell line and its derivative multidrug-resistant subline (LoVo MDR) were kindly provided by Prof. F. Majone (Department of Biology of Padova University, Italy). Cell lines were maintained in the logarithmic phase at 37 °C in a 5% carbon dioxide atmosphere using the following culture media containing 10% foetal calf serum (Euroclone, Milan, Italy), antibiotics (50 units mL^{-1} penicillin and 50 μg mL^{-1} streptomycin) and 2mM l-glutamine: (i) RPMI-1640 medium (Euroclone) for MCF-7, A431, 2008 and C13* cells; (ii) F-12 HAM'S (Sigma Chemical Co) for A549, LoVo and LoVo MDR cells. LoVo MDR culture medium also contained 0.1 μg mL^{-1} doxorubicin.

Cytotoxicity assays

The growth inhibitory effect on tumor cell lines was evaluated by means of MTT (tetrazolium salt reduction) assay.[66] Briefly, 3–8 × 10^3 cells per well, dependent upon the growth characteristics of the cell line, were seeded in 96-well microplates in growth medium (100 μL) and then incubated at 37 °C in a 5% carbon dioxide atmosphere. After 24 h, the medium was removed and replaced with a fresh one containing the compound to be studied at the appropriate concentration. Triplicate cultures were established for each treatment. After 72 h, each well was treated with 10 μL of a 5 mg mL^{-1} MTT (3-(4,5-dimethylthiazol-2-yl)-2,5-diphenyltetrazolium bromide) saline solution, and following 5 h of incubation, 100 μL of a 30 mg mL^{-1} sodium dodecylsulfate (SDS) solution in HCl 0.01 M were added. After overnight incubation, the inhibition of cell growth induced by the tested complexes was detected by measuring the absorbance of each well at 570 nm using a Bio-Rad 680 microplate reader. Mean absorbance for each drug dose was expressed as a percentage of the control untreated well absorbance and plotted *vs.* drug concentration. IC_{50} values represent the drug concentrations that reduced the mean absorbance at 570 nm to 50% of those in the untreated control wells.

Enzyme inhibition

Isolation and purification of thioredoxin reductases from rat liver cytosol and mitochondria. Highly purified cytosolic thioredoxin reductase (TrxR1) was prepared according to Luthman and Holmgren[55] starting from rat liver cytosol obtained after centrifugation of the liver homogenate at 45 000 g for 1 h. Mitochondrial thioredoxin reductase (TrxR2) was purified from liver mitochondria following the procedure of Rigobello *et al.*[67] After affinity chromatography (2′, 5′-ADP-sepharose), the enzymes were further purified by chromatography through a ω-aminohexyl-sepharose 4B column. The fractions obtained after the affinity chromatography step were concentrated by ultrafiltration and then applied on a ω-aminohexyl-sepharose 4B column equilibrated with 50 mM Tris-HCl buffer (pH 7.5) and the enzymatic fraction was eluted with a linear gradient of NaCl (from 0.0 to 0.8 M). The enzyme showed a unique band on SDS-PAGE.

***In vitro* TrxR1 and TrxR2 inhibition.** The assay was performed in 0.2 M Na, K-phosphate buffer (pH 7.4) containing 2 mM EDTA, 0.25 mM NADPH and about 0.5–2 μg of TrxR protein. The reaction was initiated by the addition of 3 mM DTNB (5,5′-dithiobis (2-nitrobenzoic acid) to both sample and reference, and the increase of absorbance was monitored at 412 nm over 5 min at 25 °C. Enzyme activity was calculated taking into account that 1 mole of NADPH yields 2 moles of CNTP anion (reduced DTNB).

***In vitro* GR inhibition.** Glutathione reductase activity was estimated at 25 °C in 0.1 M Tris/HCl (pH 8.1) containing 0.2 mM NADPH. Reactions were started by the addition of 1 mM GSSG and followed spectrophotometrically at 340 nm.

Inhibition of redox enzymes by gold(I) complexes in cells. 2008 cells were grown in 75 cm^2 flasks at confluence and treated with gold complexes at concentrations corresponding to IC_{50} values for 24 h. At the end of the incubation time, cells were collected, washed with PBS and centrifuged. Each sample was then lysed with RIPA buffer modified as follows: 150 mM NaCl, 50 mM Tris-HCl, 1% Triton X-100, 1% SDS, 1% DOC, 1 mM NaF, 1 mM EDTA, and immediately before use, an anti-protease cocktail (Roche, Basel, Switzerland) containing PMSF and supplemented with protease inhibitors was added. Samples were tested for thioredoxin reductase (0.080 mg proteins) activity as above described as well as by means of an end-point insulin assay[68] with minor modifications in order to allow 96-well plate measurements.[69] Glutathione reductase activity (0.080 mg proteins) was estimated at 25 °C in 0.1 M Tris/HCl (pH 8.1) containing 0.2 mM NADPH. Reactions were started by the addition of 1 mM GSSG and followed spectrophotometrically at 340 nm. Glutathione peroxidase activity (0.5 mg proteins) was estimated at 25 °C in 50 mM Hepes/Tris (pH 7.0) and EDTA 3 mM, 0.3 mM NADPH, 5 mM GSH and 0.25 mM tert-butyl hydroperoxide according to Little *et al.*[70]

Acknowledgements

The authors gratefully thank Dr. F. Benetollo of the C.N.R.–I.C.I.S. Institute, Padua, Italy. We are particularly indebted to the generous contribution of Prof. E. Zangrando from the Chemistry Department of University of Trieste, Italy, who allowed access to the PW1100 and DIP1030 diffractometers, supervised the X-ray data collection process and helped with the structure interpretation. The authors are grateful to CIRCSMB (Consorzio Interuniversitario per la Ricerca in Chimica dei Metalli nei Sistemi Biologici).

References

1 E. E. Trimmer and J. M. Essigmann, *Essays Biochem.*, 1999, **34**, 191–211.
2 R. Paschke, J. Kalbitz, C. Paetz, M. Luckner, T. Mueller, H.-J. Schmoll, H. Mueller, E. Sorkau and E. Sinn, *J. Inorg. Biochem.*, 2003, **94**, 335–342.
3 I. Ott and R. Gust, *Arch. Pharm.*, 2007, **340**, 117–126.
4 P. J. Barnard and S. J. Berners-Price, *Coord. Chem. Rev.*, 2007, **251**, 1889–1902.
5 A. Bindoli, M. P. Rigobello, G. Scutari, C. Gabbiani, A. Casini and L. Messori, *Coord. Chem. Rev.*, 2009, **253**, 1692–1707.
6 C. Santini, M. Pellei, G. Papini, B. Morresi, R. Galassi, S. Ricci, F. Tisato, M. Porchia, M. P. Rigobello, V. Gandin and C. Marzano, *J. Inorg. Biochem.*, 2011, **105**, 232–240.
7 O. Rackman, S. J. Nichols, P. J. Leddman, S. J. Berners Price and A. Filipovska, *Biochem. Pharmacol.*, 2007, **74**, 992–1002.
8 F. Caruso, M. Rossi, J. Tanski, C. Pettinari and F. Marchetti, *J. Med. Chem.*, 2003, **46**, 1737–1742.
9 E. Vergara, A. Casini, F. Sorrentino, O. Zava, E. Cerrada, M. P. Rigobello, A. Bindoli, M. Laguna and P. J. Dyson, *ChemMedChem*, 2010, **5**, 96–102.
10 L. Maiore, M. A. Cinellu, E. Michelucci, G. Moneti, S. Nobili, I. Landini, E. Mini, A. Guerri, C. Gabbiani and L. Messori, *J. Inorg. Biochem.*, 2011, **105**, 348–385.
11 J. S. Casas, E. E. Castellano, M. D. Couce, O. Crespo, J. Ellena, A. Laguna, A. Sànchez, J. Sordo and C. Taboada, *Inorg. Chem.*, 2007, **46**, 6236–6238.
12 E. Vergara, E. Cerrada, A. Casini, O. Zava, M. Laguna and P. J. Dyson, *Organometallics*, 2010, **29**, 2596–2603.
13 M. J. McKeage, P. Papathanasiou, G. Salem, A. Sjaarda, G. F. Swiegers, P. Waring and S. B. Wild, *Met.-Based Drugs*, 1998, **5**, 217–223.
14 S. J. Berners-Price, R. J. Bowen, P. Galettis, P. C. Healy and M. J. McKeage, *Coord. Chem. Rev.*, 1999, **185–186**, 823–836.
15 M. J. Nell, M. Wagener, J. R. Zeevaart, E. Kilian, M. A. Mamo, M. Layh, M. Coyanis and C. E. van Rensburg, *Appl. Radiat. Isot.*, 2009, **67**, 1370–1376.
16 M. J. McKeage, S. J. Berners-Price, P. Galettis, R. J. Bowen, W. Brouwer, D. Ling, L. Zhuang and B. C. Baguley, *Cancer Chemother. Pharmacol.*, 2000, **46**, 343–350.
17 K. N. Kouroulis, S. K. Hadjikakou, N. Kourkoumelis, M. Kubicki, L. Male, M. Hursthouse, S. Skoulika, A. K. V. Y. Tyurin, A. V. Dolganov, E. R. Milaeva and N. Hadjiliadis, *Dalton Trans.*, 2009, 10446–10456.
18 M. A. Halcrow, *Dalton Trans.*, 2009, 2059–2073.
19 G. Yang and R. G. Raptis, *Inorg. Chem.*, 2003, **42**, 261–263.
20 M. C. Torralba, P. Ovejero, M. J. Mayoral, M. Cano, J. A. Campo, J. V. Heras, E. Pinilla and M. R. Torres, *Helv. Chim. Acta*, 2004, **87**, 250–263.
21 H. H. Murray, R. G. Raptis and J. P. Fackler Jr., *Inorg. Chem.*, 1988, **27**, 26–33.
22 S. J. Kim, S. Kang, K. M. Park, H. Kim, W.-C. Zin, M.-G. Choi and K. Kim, *Chem. Mater.*, 1998, **10**, 1889–1893.
23 J. Barberá, A. Elduque, R. Giménez, F. J. Lahoz, J. A. López, L. A. Oro and J. L. Serrano, *Inorg. Chem.*, 1998, **37**, 2960–2967.
24 G. Yang, J. R. Martínez and R. G. Raptis, *Inorg. Chim. Acta*, 2009, **362**, 1546–1552.
25 A. A. Mohamed, T. Grant, R. J. Staples and J. P. Fackler Jr., *Inorg. Chim. Acta*, 2004, **357**, 1761–1766.
26 H. H. Murray, R. G. Raptis and J. P. Fackler Jr., *Inorg. Chem.*, 1988, **27**, 26–33.
27 K. Nomiya, R. Noguchi, K. Oshawa, K. Tsuda and M. Oda, *J. Inorg. Biochem.*, 2000, **78**, 363–370.
28 P. Ovejero, M. J. Mayoral, M. Cano and M. C. Lagunas, *J. Organomet. Chem.*, 2007, **692**, 1690–1697.

29 K. Nomiya, R. Noguchi, K. Oshawa and K. Tsuda, *J. Chem. Soc., Dalton Trans.*, 1998, 4101–4108.
30 B. Bovio, F. Bonati, A. Burini and B. R. Pietroni, *Z. Naturforsch., B: Anorg. Chem. Org. Chem.*, 1984, **39B**, 1747–1754.
31 K. Nomiya, K. Tsuda, Y. Tanabe and H. Nagano, *J. Inorg. Biochem.*, 1998, **69**, 9–14.
32 F. Bonati, A. Burini, B. R. Pietroni and E. Giorgini, *Inorg. Chim. Acta*, 1987, **137**, 81–85.
33 B. Bovio, S. Calogero, F. E. Wagner, A. Burini and B. R. Pietroni, *J. Organomet. Chem.*, 1994, **470**, 275–283.
34 O. Elbierami, M. D. Rashdan, V. Nesterov and M. A. Rawashdeh-Omary, *Dalton Trans.*, 2010, **39**, 9465–9468.
35 A. S. Humphreys, A. Filipovska, S. J. Berners Price, G. A. Koutsantonis, B. W. Skelton and A. H. White, *Dalton Trans.*, 2007, 4943–4950.
36 A. K. Rundlöf and E. S. Arnér, *Antioxid. Redox Signaling*, 2004, **6**, 41–52.
37 S. S. W. Jackson-Rosario, *Metallomics*, 2010, **2**, 112–116.
38 C. Marzano, V. Gandin, A. Folda, G. Scutari, A. Bindoli and M. P. Rigobello, *Free Radical Biol. Med.*, 2007, **42**, 872–881.
39 M. J. Mayoral, P. Ovejero, J. A. Campo, J. V. Hera, E. Pinilla, M. R. Torres, C. Lodeiro and M. Cano, *Dalton Trans.*, 2008, 6912–6924.
40 J. P. Charles, *The Aldrich Library of Infrared Spectra*, edition III, p. 1181.
41 C. F. Macrae, I. J. Bruno, J. A. Chisholm, P. R. Edgington, P. McCabe, E. Pidcock, L. Rodriguez–Monge, R. Taylor, J. van de Streek and P. A. Wood, *J. Appl. Crystallogr.*, 2008, **41**, 466–470.
42 F. H. Allen, *Acta Crystallogr., Sect. B: Struct. Sci.*, 2002, **58**, 380–388.
43 H. Duan, S. Sengupta, J. L. Petersen, N. G. Akhmedov and X. Shi, *J. Am. Chem. Soc.*, 2009, **131**, 12100–12102.
44 J. R. Lechat, R. H. de Almeida Santos, G. Banditelli and F. Bonati, *Cryst. Struct. Commun.*, 1982, **11**, 471–477.
45 R. M. Claramunt, P. Cornago, M. Cano, J. V. Heras, M. L. Gallego, E. Pinilla and M. R. Torres, *Eur. J. Inorg. Chem.*, 2003, 2693–2704.
46 K. Nomiya, R. Noguchi and M. Oda, *Inorg. Chim. Acta*, 2000, **298**, 24–32.
47 M. L. Gallego, P. Ovejero, M. Cano, J. V. Heras, J. A. Campo, E. Pinilla and M. R. Torres, *Eur. J. Inorg. Chem.*, 2004, 3089–3098.
48 V. Gandin, A. P. Fernandes, M. P. Rigobello, B. Dani, F. Sorrentino, F. Tisato, M. Bjoernstedt, A. Bindoli, A. Sturaro, R. Rella and C. Marzano, *Biochem. Pharmacol.*, 2010, **79**, 90–101.
49 Y. Zhou, X. L. Ling, S. W. Li, X. Q. Li and B. Yan, *J. Gastroenterol.*, 2010, **16**, 2291–2297.
50 Z. Liu, M. Qiu, Q. L. Tang, M. Liu, N. Lang and F. Bi, *Chin. J. Cancer.*, 2010, **29**, 661–667.
51 Y. H. Zhang, Q. Wu, X. Y. Xiao, D. W. Li and X. P. Wang, *Cancer Lett.*, 2010, **291**, 76–82.
52 C. Wersinger, G. Rebel and I. H. Lelong-Rebel, *Amino Acids*, 2000, **19**, 667–685.
53 S. Nobili, E. Mini, I. Landini, C. Gabbiani, A. Casini and L. Messori, *Med. Res. Rev.*, 2010, **30**, 550–580.
54 M. Luthman and A. Holmgren, *Biochemistry*, 1982, **21**, 6628–6633.
55 Q.-A. Sun, Y. Wu, F. Zappacosta, K.-T. Jeang, B. J. Lee, D. L. Hatfield and V. N. Gladyschev, *J. Biol. Chem.*, 1999, **274**, 24522–24530.
56 R. Rubbiani, I. Kitanovic, H. Alborzinia, S. Can, A. Kitanovic, L. A. Onambele, M. Stefanopoulou, Y. Geldmacher, W. S. Sheldrick, G. A. Prokop, S. Wolfl and I. Ott, *J. Med. Chem.*, 2010, **53**, 8608–8618.
57 R. Ladenstein, O. Epp, K. Bartels, A. Jones, R. Huber and A. Wendel, *J. Mol. Biol.*, 1979, **134**, 199–218.
58 F. G. Mann, A. F. Wells and D. Purdie, *J. Chem.Soc.*, 1937, 1828–1836.
59 J. W. A. M. Janssen, H. J. Koeners, C. G. Kruse and C. L. Habbaken, *J. Org. Chem.*, 1973, **38**, 1777.
60 A. T. C. North, D. C. Philips and F. S. Mathews, *Acta Crystallogr., Sect. A: Cryst. Phys., Diffr., Theor. Gen. Crystallogr.*, 1968, **24**, 351–359.
61 S. Parkin, B. Moezzi and H. Hope, *J. Appl. Crystallogr.*, 1995, **28**, 53–56.
62 A. Altomare, M. C. Burla, M. Camalli, G. L. Cascarano, C. Giacovazzo, A. Guagliardi, A. G. Moliterni, G. Polidori and R. Spagna, *J. Appl. Crystallogr.*, 1999, **32**, 115–119.
63 SHELXTL/NT, Version 5.10; Bruker AXS Inc., Madison, WI, 1999; G. M. Sheldrick, *Acta Crystallogr., Sect. A: Found. Crystallogr.*, 1990, **46**, 467–473.
64 G. M. Sheldrick, *Acta Cryst.*, 2008, **A64**, 112–122.
65 O. V. Dolomanov, L. J. Bourhis, R. J. Gildea, J. A. K. Howard and H. Puschmann, *J. Appl. Crystallogr.*, 2009, **42**, 339–341.
66 M. C. Alley, D. A. Scudiero, A. Monks, M. L. Hursey, M. J. Czerwinski, D. L. Fine, B. J. Abbott, J. G. Mayo, R. H. Shoemaker and M. R. Boyd, *Cancer Res.*, 1988, **48**, 589–601.
67 M. P. Rigobello, M. T. Callegaro, E. Barzon, M. Benetti and A. Bindoli, *Free Radical Biol. Med.*, 1998, **24**, 370–376.
68 A. Holmgren and M. Björnstedt, *Methods Enzymol.*, 1995, **252**, 199–208.
69 M. Selenius, A. P. Fernandes, O. Brodin, M. Björnstedt and A. K. Rundlöf, *Biochem. Pharmacol.*, 2008, **75**, 2092–2099.
70 C. Little, R. Olinescu, K. G. Reid and P. J. O'Brien, *J. Biol. Chem.*, 1970, **245**, 3632–3636.

